Materials and Structures (2016) 49:5183–5193
DOI 10.1617/s11527-016-0853-1

ORIGINAL ARTICLE

Differential-scheme based micromechanical framework for saturated concrete repaired by the electrochemical deposition method

Qing Chen · Zhengwu Jiang · Zhenghong Yang · Hehua Zhu · J. Woody Ju · Zhiguo Yan · Yaqiong Wang

Received: 30 December 2015 / Accepted: 14 March 2016 / Published online: 17 March 2016

Abstract Based on our latest work, a differential-scheme based micromechanical framework is presented to predict the properties of saturated concrete repaired by the electrochemical deposition method (EDM), which investigates the healing mechanism of the EDM at the micro-scale level theoretically and quantitatively. The three different states of the healing process, including no healing, partial healing and complete healing, are quantitatively investigated by modifying the differential-scheme and the generalized self-consistent method based on the multiphase micromechanical healing model which we presented recently. Modification procedures are utilized to rationalize the differential-scheme based estimations by considering the water effects (including further hydration and viscosity in pores) and the shapes of the pores in the concrete. Furthermore, our predictions are compared with those of the existing models and available experimental results, thus illustrating the feasibility and capability of the proposed differential-scheme based micromechanical framework. Meanwhile, it is found that the predictions in this extension correspond to the experimental data better than those of our recent work.

Keywords Electrochemical deposition method · Concrete healing · Differential-scheme · Micromechanical framework · Saturated concrete · Effective properties

Q. Chen · Z. Jiang (✉) · Z. Yang
Key Laboratory of Advanced Civil Engineering Materials of Ministry of Education, Tongji University, 1239 Siping Road, Shanghai 200092, China
e-mail: 13585546170@163.com

Q. Chen · Y. Wang
Shaanxi Provincial Major Laboratory for Highway Bridge and Tunnel, Chang'an University, Xi'an 710064, Shaanxi, China

H. Zhu · Z. Yan
State Key Laboratory for Disaster Reduction in Civil Engineering, Tongji University, 1239 Siping Road, Shanghai 200092, China

H. Zhu · Z. Yan
Key Laboratory of Geotechnical and Underground Engineering of the Ministry of Education, Tongji University, 1239 Siping Road, Shanghai 200092, China

J. W. Ju
Department of Civil and Environmental Engineering, University of California, Los Angeles, CA 90095, USA

1 Introduction

It is critically important to repair concrete cracks, which seriously deteriorate concrete's strength, performance and durability [1]. As a promising approach to repair the concrete cracks, electrochemical deposition method (EDM) has been applied to marine structures or other situations in which the traditional repairing methods are not adequate [2–5]. The healing effects of this method are due to the fact that the electrochemical deposition products can fill the (micro-)cracks and (micro-)voids in the concrete [2–18]. During the past 20 years, numerous works have been conducted on the EDM, which include different ways to produce damaged specimens, factors influencing the healing effectiveness of the EDM and assessing methods on the healing effectiveness [2–18]. However, existing literatures mainly focus on the experimental procedures, and few studies have disclosed the healing mechanism of the EDM with rigorous analytical models, particularly the micromechanical models at the microstructural level. To address these issues, the authors have recently proposed micromechanical models for saturated concrete repaired by the EDM [19]. Specifically, the healed saturated concrete is described at the micro level and represented by a three-phase composite made up of the water, the deposition products and the intrinsic concrete. Meanwhile, the Mori–Tanaka method based multilevel homogenization scheme is utilized to predict the effective properties of the saturated concrete during the healing process [19].

As an extension of our latest works [19, 20], a differential-scheme based micromechanical framework is proposed to quantitatively characterize and predict the mechanical performance of concrete healed by the EDM in this paper. Three different states of the healing process, including no healing, partial healing and complete healing, are quantitatively investigated by incorporating the differential-scheme and the generalized self-consistent method together based on the multiphase healing model we presented recently. The rest of this paper is organized as follows. Section 2 introduces the differential-scheme for the two-phase composite. The effective properties at three different states of the healing process are quantitatively predicted by modifying the differential-scheme for saturated concrete repaired by EDM. Meanwhile, modification procedures are adopted to consider the water effects and shapes of the pores in the healed concrete in Sect. 3. Numerical examples including experimental validations and comparisons with existing micromechanical models are presented in Sect. 4. Some conclusions are reached in the final section.

2 The differential-scheme for two-phase composite

2.1 The effective properties of a composite

One goal of continuum micromechanics is to estimate the effective elastic properties of a material defined over the representative volume element (RVE). The RVE is based on a ‘mesoscopic’ length scale, which is considerably larger than the characteristic length scale of particles (inhomogeneities) but smaller than the characteristic length scale of a macroscopic specimen [21]. Take a two-phase composite as an example, the effective elastic stiffness tensor **D** of the composite is defined through

$$\bar{\boldsymbol{\sigma}} = \mathbf{D} : \bar{\boldsymbol{\varepsilon}} \tag{1}$$

with

$$\bar{\boldsymbol{\sigma}} \equiv \frac{1}{V}\int_{V} \boldsymbol{\sigma}(\mathbf{x})\mathrm{d}\mathbf{x} = \frac{1}{V}\left[\int_{V_0} \boldsymbol{\sigma}(\mathbf{x})\mathrm{d}\mathbf{x} + \int_{V_1} \boldsymbol{\sigma}(\mathbf{x})\mathrm{d}\mathbf{x}\right] \tag{2}$$

$$\bar{\boldsymbol{\varepsilon}} \equiv \frac{1}{V}\int_{V} \boldsymbol{\varepsilon}(\mathbf{x})\mathrm{d}\mathbf{x} = \frac{1}{V}\left[\int_{V_0} \boldsymbol{\varepsilon}(\mathbf{x})\mathrm{d}\mathbf{x} + \int_{V_1} \boldsymbol{\varepsilon}(\mathbf{x})\mathrm{d}\mathbf{x}\right] \tag{3}$$

where V is the volume of an RVE, V_0 is the volume of the matrix, and V_1 is the volume of the inhomogeneity; $\bar{\boldsymbol{\sigma}}$ and $\bar{\boldsymbol{\varepsilon}}$ are volume averaged stress and strain of the RVE, respectively.

2.2 The differential scheme

In terms of the inclusion-based micromechanical theory and the average stress method [21–24], the effective elastic stiffness tensor of the two-phase composite can be rephrased as Eq. (4):

$$\mathbf{D} = \mathbf{D}_0 + \phi(\mathbf{D}_\mathrm{I} - \mathbf{D}_0)\mathbf{A} \tag{4}$$

where $\mathbf{D_0}$ is the elastic stiffness tensor of the matrix phase, $\mathbf{D}_\mathrm{I}$ is the elastic stiffness tensor of the inhomogeneity, **A** is the strain concentration tensor for the inhomogeneity; ϕ denotes the volume fraction of the inhomogeneity.

Let us define $\phi = \Omega_1/(\Omega_0 + \Omega_1)$ and $\phi + \Delta\phi = (\Omega_1 + \Delta\Omega)/(\Omega_0 + \Omega_1 + \Delta\Omega)$, where Ω_0 and Ω_1 represent the volume of the matrix phase and the inclusion phase in the current composite, respectively; $\Delta\Omega$ denotes the increment of inclusion volume. For the differential method, a composite with the volume fraction of inclusion equal to $\phi + \Delta\phi$, can be treated as the equivalent composite with the volume fraction of inclusion equal to $\Delta\Omega/(\Omega_0 + \Omega_1 + \Delta\Omega)$. It is noted that the matrix phase in the equivalent composite is the current composite, which includes the current matrix (Ω_0) and current inclusion (Ω_1). According to Eq. (4), the effective properties of the material can be obtained [22, 23, 25, 26]

$$\mathbf{D}(\phi + \Delta\phi) = \mathbf{D}(\phi) + \frac{\Delta\Omega}{(\Omega_0 + \Omega_1 + \Delta\Omega)} (\mathbf{D}_I - \mathbf{D}(\phi))\mathbf{A}(\mathbf{D}(\phi)) \tag{5}$$

Equation (5) can be rephrased as below through the simple derivation

$$\frac{\mathbf{D}(\phi + \Delta\phi) - \mathbf{D}(\phi)}{\Delta\phi} = \frac{1}{1 - \phi}(\mathbf{D}_\mathrm{I} - \mathbf{D}(\phi))\mathbf{A}(\mathbf{D}(\phi)) \tag{6}$$

with

$$\Delta\phi = \frac{\Omega_1 + \Delta\Omega}{\Omega_0 + \Omega_1 + \Delta\Omega} - \frac{\Omega_1}{\Omega_0 + \Omega_1} = \frac{(1 - \phi)\Delta\Omega}{(\Omega_0 + \Omega_1 + \Delta\Omega)} \tag{7}$$

When $\Delta\phi \to 0$, Eq. (6) can be expressed as

$$\frac{\mathrm{d}\mathbf{D}(\phi)}{\mathrm{d}\phi} = \frac{1}{1 - \phi} \cdot (\mathbf{D}_\mathrm{I} - \mathbf{D}(\phi)) : \mathbf{A}(\mathbf{D}(\phi)) \tag{8}$$

The composite effective properties with no inclusion effects should be the same as those of the matrix phase, which implies

$$\mathbf{D}(\phi)\big|_{\phi=0} = \mathbf{D}_0 \tag{9}$$

When the Eshelby method is considered, we write

$$\mathbf{A} = \left[\mathbf{I} + \mathbf{S}\mathbf{D}(\phi)^{-1}(\mathbf{D}_\mathrm{I} - \mathbf{D}(\phi))\right]^{-1} \tag{10}$$

where $\mathbf{S}$ is Eshelby's tensor, which depends on $\mathbf{D}(\phi)$ and the shape of the inclusions; $\mathbf{I}$ defines the fourth-order isotropic identity tensor.

3 Differential-scheme based micromechanical predictions for the effective properties of saturated concrete repaired by the EDM

3.1 Micromechanical model for saturated concrete repaired by the EDM

At the micro level, the healed saturated concrete element is composed of water, the deposition products, mortar, coarse aggregates, micro-cracks, micro-voids, and the constituent interfaces [19, 20, 27, 28]. To study the deposition product's healing effects through micromechanical framework, the three traditional solid phases, including the mortar, coarse aggregates and their interfaces, are merged into one matrix phase, namely the "intrinsic" concrete, in the RVE [19, 20, 27, 28]; the deposition products and the water phase (occupying the spaces of micro-cracks and micro-voids) are accordingly considered as the inclusion phases in the saturated concrete element. Furthermore, following assumptions are adopted to set up our micromechanical model: (1) The shape of the water-filled cracks or voids within the healed concrete is spherical, (2) during the healing process the volume of the deposition products is proportional to the volume of the spherical pore, and (3) the interfaces are perfect (well bonded) between the deposition products and the intrinsic concrete matrix [19, 20, 27–30].

According to the above assumptions, a micromechanical model for the saturated concrete element healed by the EDM can be proposed, as exhibited in Fig. 1a [19]. The equivalent inclusion can be obtained by homogenization of the two-phase composite made up of the water and the deposition products, as shown in Fig. 1b. During the healing process of saturated concrete, the water phase is replaced by the deposition products phase. By predicting the effective properties using our micromechanical model, the mechanical performance of the concrete can be quantitatively assessed during the healing process. Different with our recent work [19, 20, 27, 28], a differential-scheme based homogenization process is utilized to obtain the properties of the healed saturated concrete according to [31–45]. Furthermore, three different states of the healing process, including no healing, partial healing and complete healing, are quantitatively investigated based on our proposed multiphase healing model.

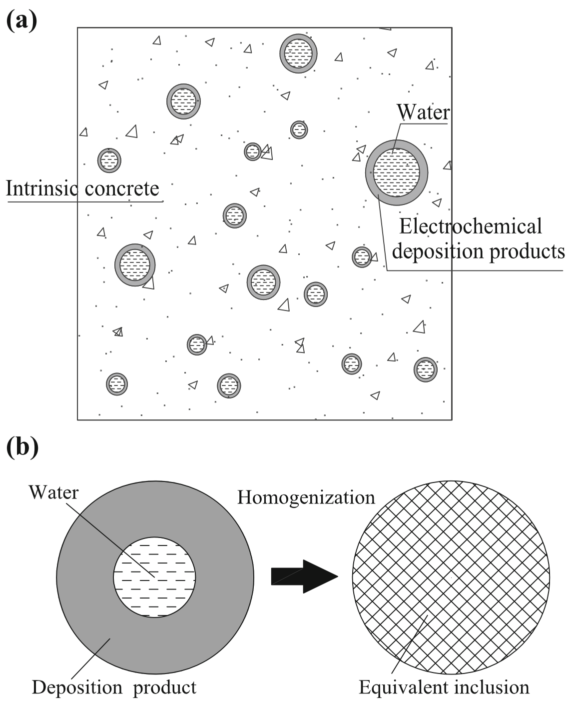

Fig. 1 Micromechanical representations: **a** the multiphase micromechanical model for saturated concrete healed by the EDM; **b** the equivalent inclusion

3.2 The effective properties of saturated healed concrete at two extreme states

The first extreme state is that there is no electrochemical deposition product (no healing process) in the concrete at all (which is equal to a saturated concrete). Therefore, the only inclusion phase in our proposed model is water itself. Let $\mathbf{D}_1$ and $\mathbf{D}_3$ represent the stiffness tensor of the water phase and the intrinsic concrete; Let $\mathbf{D}_{e1}$ be the stiffness tensor of the equivalent composite of the saturated concrete predicted by the differential scheme; ϕ_F denote the volume fraction of water in the saturated concrete. For the isotropic matrix and spherical equivalent inclusions, the tensorial components of $\mathbf{I}$, $\mathbf{D}_1$, $\mathbf{D}_3$, and $\mathbf{D}_{e1}$ are as follows:

$$I_{ijkl} = \frac{1}{3}\delta_{ij}\delta_{kl} + \frac{1}{2}\left(\delta_{ik}\delta_{jl} + \delta_{il}\delta_{jk} - \frac{2}{3}\delta_{ij}\delta_{kl}\right) \quad (11)$$

$$D_{3ijkl} = K_3\delta_{ij}\delta_{kl} + \mu_3\left(\delta_{ik}\delta_{jl} + \delta_{il}\delta_{jk} - \frac{2}{3}\delta_{ij}\delta_{kl}\right) \quad (12)$$

$$D_{1ijkl} = K_1\delta_{ij}\delta_{kl} + \mu_1\left(\delta_{ik}\delta_{jl} + \delta_{il}\delta_{jk} - \frac{2}{3}\delta_{ij}\delta_{kl}\right) \quad (13)$$

$$D_{e1ijkl} = K_{e1}\delta_{ij}\delta_{kl} + \mu_{e1}\left(\delta_{ik}\delta_{jl} + \delta_{il}\delta_{jk} - \frac{2}{3}\delta_{ij}\delta_{kl}\right) \quad (14)$$

where δ_{ij} is the Kronecker delta. K_3, μ_3 (K_1, μ_1) are respectively the bulk modulus and shear modulus of the intrinsic concrete (water), and K_{e1}, μ_{e1} are those of the equivalent composite of the saturated concrete predicted by the differential scheme, correspondingly.

By replacing the matrix phase and inhomogeneities (inclusion phase) with the intrinsic concrete and water, the differential-scheme is modified to obtain the effective properties of the saturated concrete. By substituting Eqs. (11)–(14) into Eqs. (8)–(10), the effective bulk modulus and shear modulus of the saturated concrete are obtained by solving the following nonlinear ordinary differential equations after some derivations:

$$\frac{dK_{e1}}{d\phi_F} + \frac{(K_{e1} - K_1)(3K_{e1} + 4\mu_{e1})}{(1 - \phi_F)(3K_1 + 4\mu_{e1})} = 0 \quad (15)$$

$$\frac{d\mu_{e1}}{d\phi_F} + \frac{5\mu_{e1}(\mu_{e1} - \mu_1)(3K_{e1} + 4\mu_{e1})}{(1 - \phi_F)[3K_{e1}(3\mu_{e1} + 2\mu_1) + 4\mu_{e1}(2\mu_{e1} + 3\mu_1)]} = 0 \quad (16)$$

When the porosity is zero, the properties of the saturated concrete should be equal to those of intrinsic concrete, which implies the initial conditions as below

$$K_{e1}(0) = K_3 \quad (17)$$

$$\mu_{e1}(0) = \mu_3 \quad (18)$$

The second extreme state is that the saturated concrete has been completely healed by the EDM. Therefore, the healed concrete is effectively a two-phase composite with isotropic spherical deposition products as the inclusion phase. Suppose that K_{e2} and μ_{e2} (K_2 and μ_2) are the bulk modulus and shear modulus of the completely healed concrete (deposition products). By respectively replacing K_{e1}, μ_{e1} and K_1, μ_1 in Eqs. (15)–(18) with K_{e2}, μ_{e2} and K_2, μ_2, the effective properties of completely healed concrete can be similarly achieved with the differential scheme, which can be expressed as below

$$\frac{dK_{e2}}{d\phi_F}+\frac{(K_{e2}-K_2)(3K_{e2}+4\mu_{e2})}{(1-\phi_F)(3K_2+4\mu_{e2})}=0 \tag{19}$$

$$\frac{d\mu_{e2}}{d\phi_F}+\frac{5\mu_{e2}(\mu_{e2}-\mu_2)(3K_{e2}+4\mu_{e2})}{(1-\phi_F)[3K_{e2}(3\mu_{e2}+2\mu_2)+4\mu_{e2}(2\mu_{e2}+3\mu_2)]}=0 \tag{20}$$

with the initial conditions as below

$$K_{e2}(0)=K_3 \tag{21}$$

$$\mu_{e2}(0)=\mu_3 \tag{22}$$

3.3 The effective properties of saturated concreted partially healed by EDM

As to saturated concrete partially healed by EDM, the two inclusion phases (water and deposition products) should be taken into considerations. According to [31–45], the differential-scheme based two-level homogenization scheme is employed to attain the effective properties of the saturated healed concrete, which is a *three-phase* composite made up of the intrinsic concrete, the deposition products and the water phase. Through the first level homogenization, as shown in Fig. 1b, the equivalent inclusion can be obtained with the generalized self-consist model by modifying its inner- and outer-layer phases into the water phase and the deposition products, respectively [46, 47]. Accordingly, the effective bulk modulus and shear modulus for the equivalent inclusion can be expressed by Eqs. (23) and (24), correspondingly:

$$K_F=K_2+\frac{\phi_{FD}(K_1-K_2)\,(3K_2+4\mu_2)}{3K_2+4\mu_2+3\,(1-\phi_{FD})\,(K_1-K_2)} \tag{23}$$

$$A\left(\frac{\mu_F}{\mu_2}\right)^2+B\left(\frac{\mu_F}{\mu_2}\right)+C=0 \tag{24}$$

where ϕ_{FD} is the volume fraction of the water phase in the two-phase composite composed by the water and the deposition products. Further, K_1, K_2 and K_F(μ_1, μ_2 and μ_F) denote the bulk modulus (the shear modulus) for the water, the deposition products and the equivalent inclusion after the first level homogenization, respectively. A, B, C are parameters dependent on ϕ_{FD}, the properties of the water and those of deposition products. See details in our previous work [19, 20, 27, 28].

Let us define K_S and μ_S as the effective bulk modulus and shear modulus of the saturated healed concrete. In this differential-scheme based micromechanical framework, these two effective properties can be obtained with the second level homogenization. Specifically, by replacing K_{e1}, μ_{e1}, K_1, and μ_1 in Eqs. (15)–(18) with K_S, μ_S, K_F, and μ_F, the effective properties of the partially healed concrete (K_S and μ_S) can be calculated by solving the following nonlinear ordinary differential equations

$$\frac{dK_S}{d\phi_F}+\frac{(K_S-K_F)(3K_S+4\mu_S)}{(1-\phi_F)(3K_F+4\mu_S)}=0 \tag{25}$$

$$\frac{d\mu_S}{d\phi_F}+\frac{5\mu_S(\mu_S-\mu_F)(3K_S+4\mu_S)}{(1-\phi_F)[3K_S(3\mu_S+2\mu_F)+4\mu_S(2\mu_S+3\mu_F)]}=0 \tag{26}$$

with the initial conditions as below

$$K_S(0)=K_3 \tag{27}$$

$$\mu_S(0)=\mu_3 \tag{28}$$

With the bulk modulus and shear modulus, the material's Young's modulus and Poisson's ratio can be computed from the following well-known expression:

$$E=\frac{9K\mu}{3K+\mu} \tag{29}$$

$$v=\frac{1-2\mu/3K}{2+2\mu/3K} \tag{30}$$

where K, μ, E and v are the material bulk modulus, shear modulus, Young's modulus and Poisson's ratio, respectively.

3.4 Modifications to the differential-scheme based predictions

The following two procedures are performed to consider the water effects. On one hand, further hydration occurs when the concrete is saturated [48, 49]. Like previous works [19, 20, 48, 49], ϕ_F in Eqs. (15)–(16) and Eqs. (25)–(26) should be replaced by the effective porosity of saturated concrete $\phi_{EF}=m\phi_F$ to consider these impacts, where m is a coefficient, and $m<1$. On the other hand, the water viscosity improves the shear modulus of the concrete [48, 49]. The similar function $f(\phi_F) = a\,\phi_F^2 + b\,\phi_F + 1$ from [19, 20, 48, 49] is adopted to modify the micromechanical estimations of the shear modulus [19, 49]. See details in [19, 49].

The pores can't be assumed to be spherical any more for the dried specimen [19, 20, 29, 49]. From the view point of micromechanics, (micro-)cracks or (micro-)voids within concrete can be classified as ''stiff'' pores and ''soft'' pores, respectively. The former can be represented as a sphere, and the latter can be signified as an ellipse or a disk, which generally decrease the stiffness of the concrete [19, 20, 29, 49]. All pores in the saturated concrete are assumed to be spherical since the water is able to resist the deformations of the specimen [19, 20, 29, 49]. However, this assumption is not reasonable when the specimen is dried; i.e., the influence of the pore shape should be considered [19, 20, 29, 49]. Based on [19, 50], three modification coefficients, χ_K, χ_μ and χ_E, are similarly employed in the extension:

$$\chi_K = \frac{K_\alpha^*}{K_{\alpha=1}^*} \tag{31}$$

$$\chi_\mu = \frac{\mu_\alpha^*}{\mu_{\alpha=1}^*} \tag{32}$$

$$\chi_E = \frac{E_\alpha^*}{E_{\alpha=1}^*} \tag{33}$$

$$\alpha = \frac{1}{N}\sum_{i=1}^{N}\frac{a_i}{b_i} \tag{34}$$

where a_i and b_i are the lengths of the pores' minor and major axes, respectively, and N is the number of different pores within the concrete specimens; α is the equivalent aspect ratio; $K_{\alpha=1}^*$, $\mu_{\alpha=1}^*$ and $E_{\alpha=1}^*$ (K_α^*, μ_α^* and E_α^*) are respectively the predicted effective bulk modulus, the effective shear modulus and Young's modulus, when $\alpha = 1$ ($\alpha < 1$). The effective properties $K_{\alpha=1}^*$, $\mu_{\alpha=1}^*$, $E_{\alpha=1}^*$, K_α^*, μ_α^* and E_α^* of the dry healed concrete can be obtained using the micromechanical iteration schemes [50]. See details in [19, 50].

It is noted that Eqs. (37)–(43) in [19] are derived based on the assumption that the properties of deposition products and intrinsic concrete are the same with each other. The homogenization process should be utilized when this assumption does not hold. It implies that K_2 and μ_2 in Eqs. (37)–(43) of [19] should be replaced by K_{av} and μ_{av}, which are obtained by the following expressions:

$$K_{av} = 0.5\,[\phi_G K_2 + (1-\phi_G)K_3] + 0.5\left[\frac{K_2 K_3}{\phi_G K_3 + (1-\phi_G)K_2}\right] \tag{35}$$

$$\mu_{av} = 0.5\,[\phi_G \mu_2 + (1-\phi_G)\mu_3] + 0.5\left[\frac{\mu_2 \mu_3}{\phi_G \mu_3 + (1-\phi_G)\mu_2}\right] \tag{36}$$

$$\phi_G = \frac{V_{de}}{V_{de} + V_{in}} \tag{37}$$

where K_{av}, μ_{av} are the effective bulk modulus and shear modulus of the equivalent material made up of the deposition products and the intrinsic concrete. ϕ_G is the volume fraction of the deposition product in the equivalent composite; V_{de} and V_{in} are the volume of deposition products and intrinsic concrete.

So the effective properties of the healed saturated concrete in the dry state can be obtained as follows: Firstly, the properties of water should be replaced by those of air in the first step homogenization; secondly, the water viscosity in pores should be ignored in the second step homogenization; thirdly, with the results calculated by Eqs. (37)–(43) of [19], the properties of the healed saturated concrete in the dry state can be obtained by multiplying the results of the second step homogenization and the modifying coefficients obtained with Eqs. (31)–(34).

Furthermore, if the nondestructive testing methods, such as the ultrasonic waves, are employed to test the effective dynamic properties of concrete repaired by the EDM, the static properties should be modified into dynamic properties according to the relationships between the two types [19, 51].

4 Verifications

4.1 Comparisons with experiments and existing models of the EDM

Our predictions are compared with the experimental data and the estimations of the existing models to verify the capacity of the proposed differential-scheme based micromechanical framework for saturated concrete repaired by the EDM.

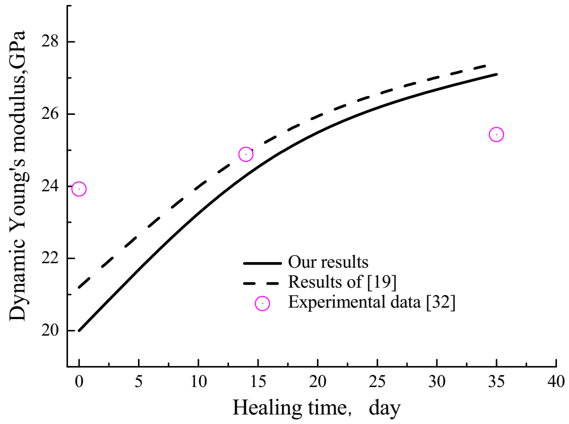

Fig. 2 The comparisons among our predictions, results of [19] and those obtained experimentally [28]

Firstly, with the modifications in Sect. 3.4, the differential-scheme based micromechanical model for the healed saturated concrete can be modified to predict the properties of the healed specimen when they are dried. Here, the dynamic Young's moduli in the dry state of the specimen before and after healing in Chen's experiment [28] are adopted to validate the proposed micromechanical model. The average initial porosity of the specimen is 0.299. The average pulse-velocity of its intrinsic concrete is 5134.5 m/s. The density is 2537.9 kg/m^3 and the Poisson's ratio is 0.229. As exhibited in Fig. 2, the predictions obtained from the micromechanical model correspond well with those obtained experimentally with the maximum relative difference between the experimental data and our results being 16.3 %. Overall, the predictions in this paper are still close to those of Zhu et al. [19].

Table 1 Properties of three types of deposition products [19]

	Bulk modulus (GPa)	Shear modulus (GPa)
Type 1	18.61	12.3
Type 2	27.91	18.45
Type 3	41.865	26.675

Table 2 Properties of intrinsic concrete and water [19]

Properties	Bulk modulus (GPa)	Shear modulus (GPa)
Intrinsic concrete	27.91	18.45
Water	2.25	0

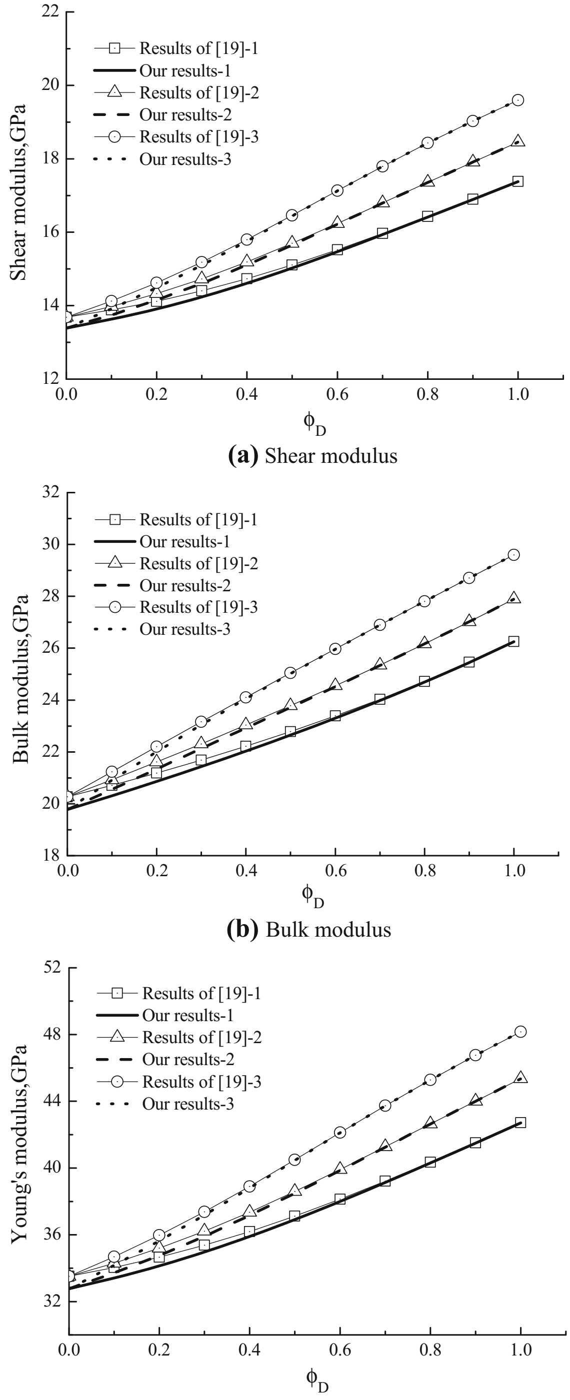

(a) Shear modulus

(b) Bulk modulus

(c) Young's modulus

Fig. 3 The comparisons of mechanical properties between our predictions and those of Zhu et al. [19] with ϕ_D denoting the volume fraction of deposition products in the equivalent inclusion, −1, −2 and −3 representing the results obtained with the first, second and third type of deposition products, respectively

Secondly, the existing models [19] are utilized to verify our proposed differential-scheme based micromechanical framework. The predicting results of the different models are compared using three types of deposition products, whose properties are listed in Table 1 [19]. The properties of the intrinsic concrete and water are listed in Table 2 according to [19].

Figure 3a–c present the comparisons of mechanical properties between our predictions and those of [19] during healing process. From Fig. 3a, it can be observed that our predictions for the shear modulus of the equivalent composite are very close to those of [19], which means our proposed differential-scheme based micromechanical model is also capable of describing the healing process from the micro-scale level. Meanwhile, the results of the two different micromechanical models show that the values of effective shear modulus gradually increase during the healing process due to the accumulation of deposition products. The stronger the deposition product is, the greater the equivalent composite becomes during the healing process. As to the effective bulk modulus and Young's modulus, predictions in this paper are also similar to those obtained by [19], which are exhibited by Fig. 3b, c, respectively. Moreover, the properties of the deposition products still play an important role in the mechanical properties of the concrete during the healing process.

Thirdly, the Voigt upper bound and Reuss lower bound [22, 23] of the effective properties of concrete during the healing process are employed to validate our predictive results. Figure 4a, b present the comparisons among the results obtained with the proposed micromechanical model, the Voigt lower bounds and the Reuss upper bounds during the healing process for the effective properties. It can be found from Fig. 4a that the predictions of the shear modulus of the healed concrete lie between the upper and lower bounds reasonably. When the bulk modulus are considered, similar conclusions can be reached in Fig. 4b.

In summary, the comparisons between our predicting results and those obtained experimentally, and those reached by the existing models show that the proposed differential-scheme based micromechanical model can quantitatively describe the healing process reasonably well at the micro-scale level.

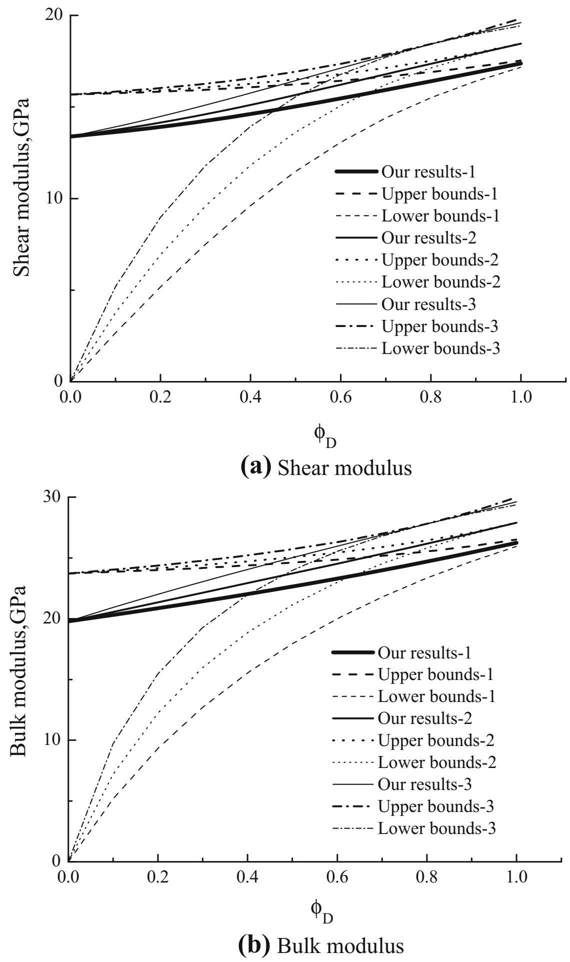

Fig. 4 The comparisons among the results obtained with the proposed micromechanical model, the Voigt lower bounds and the Reuss upper bounds during the healing process for the effective properties, with ϕ_D denoting the volume fraction of deposition products in the equivalent inclusion, −1, −2 and −3 representing the results obtained with the first, second and third type of deposition products, respectively

4.2 Comparison with experiments and existing models at two extreme states of the EDM

In this section, our predictions at two extreme states of the EDM are examined to further validate the proposed differential-scheme based micromechanical framework.

The first extreme state is that there is absolutely no healing process in the concrete. Figure 5 exhibits the comparisons among our results, those obtained by [19], the upper bounds, lower bounds and the experimental data of Yaman et al. [52]. The comparison

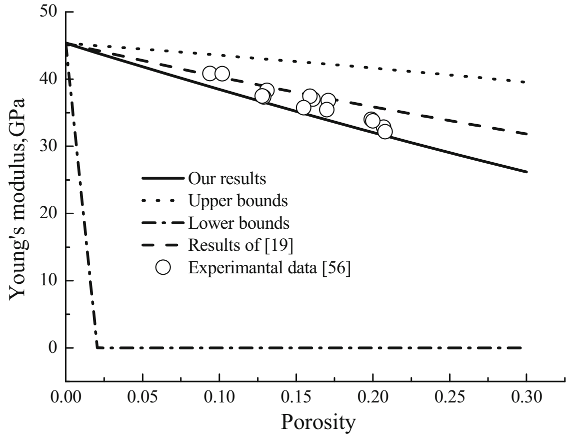

Fig. 5 The comparison among the results obtained with the different micromechanical models and those obtained experimentally for the static Young's modulus of saturated concrete

shows that our predictions and those of Zhu et al. [19] agree well with the experimental data when the porosity is low. These two predictions are between the upper bounds and lower bounds reasonably. With the increase of the porosity, our predictions correspond with the experimental data better than those of Zhu et al. [19].

The second extreme state is that the saturated concrete has been completely healed by the EDM. Therefore, there is no water effect and the healed concrete is effectively a two-phase composite with the isotropic spherical inclusion phase. The works done by Smith [53] are employed to verify our proposed model at the second extreme state. Figures 6 and 7 present

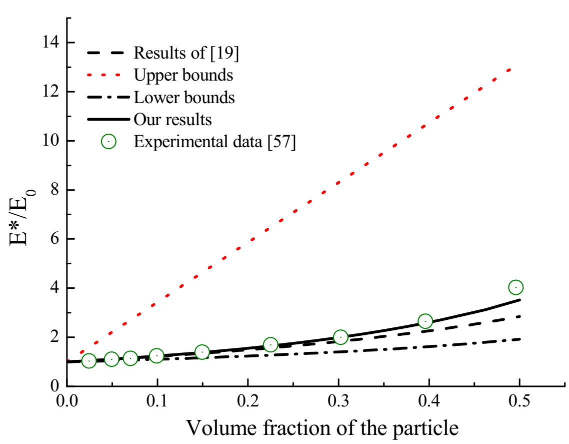

Fig. 6 The comparisons among our results, those obtained by Zhu et al. [19], the upper bounds, the lower bounds and the experimental data of Smith [53] for the Young's modulus of two-phase composite

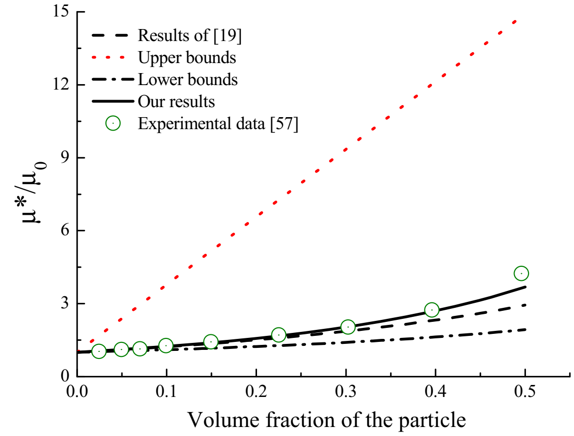

Fig. 7 The comparisons among our results, those obtained by Zhu et al. [19], the upper bounds, the lower bounds and the experimental data of Smith [53] for the shear modulus of two-phase composite

the comparisons among our results, those obtained by Zhu et al. [19], the upper bounds, the lower bounds and the experimental data of Smith [53]. From Fig. 6, it can be found that our predictions for the Young's modulus and those of Zhu et al. [19] agree well with the experimental data when the volume fraction of the particle is low. These two predictions lie between the upper bounds and lower bounds reasonably. However, our predictions correspond much better with the experimental data than those of Zhu et al. [19] when the volume fraction of the particle increases to 0.4–0.5. Similar conclusion can be reached when the shear modulus is considered according to Fig. 7.

In summary, our proposed differential-scheme based micromechanical framework for saturated concrete repaired by the EDM can predict the properties of the saturated concrete or the spherical particle reinforced composite at the extreme states. Compared with the previous models [19], the predictions of this new framework agree well with the experimental data better when the volume fraction of the inclusion is higher.

5 Conclusions

The EDM is a newly developed healing method for cracked concrete under a water environment. Many meaningful experimental studies have been performed to evaluate its healing effectiveness. However, there are limited theoretical models, especially the micromechanical models, available for describing the healing process of the concrete repaired by the EDM at the micro-scale level. As an extension of our latest work, the differential-scheme based micromechanical framework is proposed in this paper to quantitatively describe the healing process of concrete healed by the EDM. Three different states for the healing process are quantitatively investigated with different types of deposition products. Furthermore, our predictions are compared with those of the existing micromechanical models and the experimental data. The following conclusions can be reached:

(1) The proposed differential-scheme based micromechanical models can quantitatively predict the mechanical properties of saturated concrete repaired by the EDM during the entire healing process. As a special case, the micromechanical framework can accurately estimate the effective properties of two-phase composites, including the saturated concrete.
(2) The deposition products properties play an important role in determining the mechanical properties of concrete during the healing process. With the increase of the bulk modulus or shear modulus of the deposition products, the healed saturated concrete will enjoy higher mechanical properties.
(3) Compared with the results of our latest models, the estimations of this differential-scheme based framework agree well with the experimental data better when the volume fraction of the inclusion is higher.

It is noted that the concrete element is assumed to be fully saturated for simplifications in this paper [19]. Actually concrete pores are rarely saturated in practice. With the decrease of the saturation degree, the mechanical performance of the healed specimen will reduce. See details for [54].

Acknowledgments This work is supported by the National Key Basic Research and Development Program (973 Program, No. 2011CB013800) and National Natural Science Foundation of China (51508404, 51478348, 51278360, 51308407). This work is also supported by the 1000 Talents Plan Short-Term Program by the Organization Department of the Central Committee of the CPC, Research Program of State Key Laboratory for Disaster Reduction in Civil Engineering, the Scientific Platform Open Funds of Fundamental Research Plan for the Central Universities, Chang'an University (310821151113) and Natural Science Foundation of Shandong Province (ZR2013EEL019).

References

1. Mehta PK (1997) Durability-critical issues for the future. Concr Int 19:1–12
2. Edvardsen C (1999) Water permeability and autogenous healing of cracks in concrete. ACI Mater J 96(4):448–454
3. Otsuki N, Ryu JS (2001) Use of electrodeposition for repair of concrete with shrinkage cracks. J Mater Civ Eng ASCE 13(2):136–142
4. Yokoda M, Fukute T (1992). Rehabilitation and protection of marine concrete structure using electrodeposition method. In: Proceedings of the international RILEM/CSIRO/ACRA conference on rehabilitation of concrete structures, RILEM, Melbourne, pp 213–222
5. Sasaki H, Yokoda M (1992). Repair method of marine reinforced concrete by electro deposition technique. In: Proceedings of the annual conference of Japanese Concrete Institute, pp 849–854
6. Ryu JS, Otsuki N (2002) Crack closure of reinforced concrete by electro deposition technique. Cem Concr Res 32(1):159–264
7. Ryu JS (2003) New waterproofing technique for leaking concrete. J Mater Sci Lett 22:1023–1025
8. Monteiro P, Ryu JS (2004) Electrodeposition as a rehabilitation method for concrete materials. Can J Civ Eng 31(5):776–781
9. Ryu JS, Otsuki N (2005) Experimental study on repair of concrete structural members by electrochemical method. Scripta Mater 52:1123–1127
10. Mohankumar G (2005) Concrete repair by electrodeposition. Indian Concr J 79(8):57–60
11. Ryu JS (2001) An experimental study on the repair of concrete crack by electrochemical technique. Mater Struct 34(241):433–437
12. Ryu JS, Otsuki N (2001) Rehabilitation of cracked reinforced concrete using electrodeposition method. Mater Sci Res Int 7(2):122–126
13. Chang JJ, Yeih WC, Hsu HM, Huang NM (2009) Performance evaluation of using electrochemical deposition as a repair method for reinforced concrete beams. Tech Sci Press SL 1(2):75–93
14. Jiang ZW, Xing F, Sun ZP, Wang PM (2008) Healing effectiveness of cracks rehabilitation in reinforced concrete using electrodeposition method. J Wuhan Univ Technol 23(6):917–922
15. Ryu JS (2003) Influence of crack width, cover depth, water cement ratio and temperature on the formation of electrodeposition on the concrete surface. Mag Concr Res 55(1):35–40
16. Chu HQ, Jiang LH (2009) Correlation analysis between concrete parameters and electrodeposition effect based on grey theory. J Wuhan Univ Technol 31(7):22–26
17. Otsuki N, Hisada M, Ryu JS, Banshoya EJ (1999) Rehabilitation of concrete cracks by electrodeposition. Concr Int 21(3):58–62
18. Ryu JS, Otsuki N (2002) Application of electrochemical techniques for the control of cracks and steel corrosion in concrete. J Appl Electrochem 32(6):635–639
19. Zhu HH, Chen Q, Yan ZG, Ju JW, Zhou S (2014) Micromechanical model for saturated concrete repaired by

electrochemical deposition method. Mater Struct 47:1067–1082
20. Chen Q, Zhu HH, Yan ZG, Deng T, Zhou S (2015) Micro-scale description of the saturated concrete repaired by electrochemical deposition method based on Mori–Tanaka method. J Build Struct 36(1):98–103
21. Ju JW, Chen TM (1994) Micromechanics and effective moduli of elastic composites containing randomly dispersed ellipsoidal inhomogeneities. Acta Mech 103:103–121
22. Qu JM, Cherkaoui M (2006) Fundamentals of micromechanics of solids. Wiley, Hoboken
23. Mura T (1987) Micromechanics of defects in solids. Martinus Nijhoff Publishers, Dordrecht
24. Ju JW, Chen TM (1994) Effective elastic moduli of two-phase composites containing randomly dispersed spherical inhomogeneities. Acta Mech 103:123–144
25. Norris AN (1985) A differential scheme for the effective modulus of composites. Mech Mater 4:1–16
26. McLaughlin R (1977) A study of the differential scheme for composite materials. Int J Eng Sci 15:237–244
27. Chen Q, Zhu HH, Yan ZG, Ju JW, Deng T, Zhou S (2015) Micro-scale description of the saturated concrete repaired by electrochemical deposition method based on self-consistent method. Chin J Theor Appl Mech 47(2):367–371
28. Chen Q (2014) The stochastic micromechanical models of the multiphase materials and their applications for the concrete repaired by electrochemical deposition method. Doctor dissertation of Tongji University, Shanghai
29. Stora E, He QC, Bary B (2006) Influence of inclusion shapes on the effective linear elastic properties of hardened cement pastes. Cem Concr Res 36(7):1330–1344
30. Jiang LH, Chu HQ (2005) Influence of concrete parameters on electrodeposition effect. Adv Sci Technol Water Resour 25(2):23–25
31. Li GQ, Zhao Y, Pang SS (1999) Four-phase sphere modeling of effective bulk modulus of concrete. Cem Concr Res 29:839–845
32. Garboczi EJ, Berryman JG (2001) Elastic moduli of a material containing composite inclusions: effective medium theory and finite element computations. Mech Mater 33(2):455–470
33. Yang QS, Tao X, Yang H (2007) A stepping scheme for predicting effective properties of the multi-inclusion composites. Int J Eng Sci 45:997–1006
34. Nguyen NB, Giraud A, Grgic D (2011) A composite sphere assemblage model for porous oolitic rocks. Int J Rock Mech Min Sci 48:909–921
35. Ju JW, Zhang XD (1998) Micromechanics and effective transverse elastic moduli of composites with randomly located aligned circular fibers. Int J Solids Struct 35(9–10):941–960
36. Ju JW, Sun LZ (1999) A novel formulation for the exterior-point Eshelby's tensor of an ellipsoidal inclusion. J Appl Mech 66(2):570–574
37. Ju JW, Sun LZ (2001) Effective elastoplastic behavior of metal matrix composites containing randomly located aligned spheroidal inhomogeneities. Part I: micromechanics-based formulation. Int J Solids Struct 38(2):183–201
38. Sun LZ, Ju JW (2001) Effective elastoplastic behavior of metal matrix composites containing randomly located aligned spheroidal inhomogeneities. Part II: applications. Int J Solids Struct 38(2):203–225
39. Sun LZ, Ju JW (2004) Elastoplastic modeling of metal matrix composites containing randomly located and oriented spheroidal particles. J Appl Mech 71:774–785
40. Ju JW, Yanase K (2010) Micromechanics and effective elastic moduli of particle-reinforced composites with near-field particle interactions. Acta Mech 215(1):135–153
41. Ju JW, Yanase K (2011) Micromechanical effective elastic moduli of continuous fiber-reinforced composites with near-field fiber interactions. Acta Mech 216(1):87–103
42. Yanase K, Ju JW (2012) Effective elastic moduli of spherical particle reinforced composites containing imperfect interfaces. Int J Damage Mech 21(1):97–127
43. Chen Q, Zhu HH, Ju JW, Guo F, Wang LB, Yan ZG, Deng T, Zhou S (2015) A stochastic micromechanical model for multiphase composite containing spherical inhomogeneities. Acta Mech 226(6):1861–1880
44. Zhu HH, Chen Q, Ju JW, Yan ZG, Guo F, Wang YQ, Jiang ZW, Zhou S, Wu B (2015) Maximum entropy based stochastic micromechanical model for two-phase composite considering the inter-particle interaction effect. Acta Mech 226(9):3069–3084
45. Sheng P (1990) Effective-medium theory of sedimentary rocks. Phys Rev B 41:4507–4512
46. Christensen RM, Lo KH (1979) Solutions for effective shear properties in three phase sphere and cylinder models. J Mech Phys Solids 27:315–330
47. Hashin Z (1962) The elastic moduli of heterogeneous materials. J Appl Mech 29:143–150
48. Wang HL, Li QB (2005) Saturated concrete elastic modulus prediction. J Tsinghua Univ 45(6):761–763
49. Wang HL, Li QB (2007) Prediction of elastic modulus and Poisson's ratio for unsaturated concrete. Int J Solids Struct 44:1370–1379
50. Berryman JG (1980) Long-wave propagation in composite elastic media II. Ellipsoidal inclusion. J Acoust Soc Am 68(6):1820–1831
51. Prassianakis IN, Prassianakis NI (2004) Ultrasonic testing of non-metallic materials: concrete and marble. Theor Appl Fract Mech 42:191–198
52. Yaman IO, Hearn N, Aktan HM (2002) Active and non-active porosity in concrete part I: experimental evidence. Mater Struct 35(3):102–109
53. Smith JC (1976) Experimental values for the elastic constants of a particulate-filled glassy polymer. J Res NBS 80A:45–49
54. Yan ZG, Chen Q, Zhu HH, Ju JW, Zhou S, Jiang ZW (2013) A multiphase micromechanical model for unsaturated concrete repaired by electrochemical deposition method. Int J Solids Struct 50(24):3875–3885